Spatially aggregated climate indicators over Sweden (1860–2020): Response to reviewers

Christophe Sturm[1]

[1]Swedish Meteorology and Hydrology Institute

Correspondence: Christophe Sturm (christophe.sturm@smhi.se)

Abstract.

This document presents the response to reviews on Sturm (2024b): "EOF-based climate indicators over Sweden (part 1: temperature)". Both reviews (Anonymous, 2024a, b) recommend major revisions concerning the EOF methodology: we address here previous shortcomings, present corrected results and discuss the difference to the original ones.

After a thorough review of suggested literature, we perform new analytical and numerical calculuses on the original data, and conclude that the rigorous theoretical approach reinforces the benefits of an EOF-based climate indicator to correct biases of the reference method (arithmetical averaging). We hereby express our gratitude for the reviewers' detailed comments and suggestion, enabling major improvements to the previous manuscript.

1 Introduction

The submitted manuscript (Sturm, 2024b) describes a novel method to compute a national climate indicator for temperature in Sweden since 1860, based on an EOF (Empirical Orthogonal Functions) analysis. It is followed by a companion article using the same methodology, applied on precipitation observations (Sturm, 2024a).

Both reviewers (Anonymous, 2024a, b) recommend major revisions to the submitted manuscript, which are addressed hereafter. The first review (Anonymous, 2024a) highlights a methodological flaw in the use of EOF:

'As explained in a more detailed way below, the application of the EOF-based method is not totally correct. For instance, the method described here reconstructs the expansion temporal coefficients by projecting the available station observations onto the EOF patterns. However, when restricted to the location of the available observations, the EOF patterns are not orthogonal anymore – they are only orthogonal over the full set of stations in which they were calculated.

Thus, the way to 'reconstruct' the expansion coefficients is another one in the case of gappy data, as described in the book by von Storch and Zwiers (1999) Statistical Analysis in Climate Research. I believe that this methodological error is not determinant and that the application of the correct method will yield similar results."

The second review (Anonymous, 2024b) recommends as major revisions (i) a better description of the gap-filling methodology, based on a linear regression of the "gappy" MORA dataset versus the gridded GRIDCLIM (see below), and (ii) to develop a " specific test against the geometry in the distribution of missing values".

The present response to reviewers is structured as follows. As a preliminary task, we have further developed the *theoretical fundamentals of EOF* in climate studies, following suggested bibliography references (Hannachi et al., 2023, 2007; Storch and Zwiers, 1999; Björnsson and Venegas, 1997; Preisendorfer, 1988): a succinct review is presented in the appendix. In particular, we have focussed on following relevant aspects:

- Definition of EOF as eigenvectors of the covariance matrix of the observation dataset.
- Implication of the dimension conventions for the observational dataset (i.e. $time \times space$ or $space \times time$ observation matrix) for the EOF definition – in other words, the difference between defining the EOF on the *spatial* or *time* covariance in observations.
- The estimation of EOF from a "gappy" dataset, i.e. containing missing values. This (previously overlooked) aspect enabled a major improvement to the original manuscript.

The first section focuses on a better *description of the original methodology*. The first sub-section focuses on the gap-filling methodology (based on a linear regression of the "gappy" MORA dataset versus the gridded GRIDCLIM); the second sub-section focuses on an analytical investigation on the impact of the breach of the orthogonality constraint in the original methodology.

The second section explores the *estimation of EOF from a gappy dataset*, which represents the major improvement of the revised manuscript. Following Storch and Zwiers (1999), we present in its first subsection a complementary method to estimate EOF from the gappy observation dataset, which does not require the gap-filling procedure over the 1961–2018 calibration period. In order to evaluate the impact of the "geometry in the distribution of missing values" (Anonymous, 2024b), we introduce an additional pre-processing of the observational dataset.

- While the original manuscript restricted the total 933 station time-series to 466 items over the 1961–2018 calibration period, the computation of EOF from a "gappy" dataset allows to process all 933 stations.
- The total 993 time-series included numerous duplicate stations, i.e. neighbouring stations with limited time overlap. A *merged* dataset was prepared by "stitching" (or coupling) neighbouring stations into a single synthetic time-series, reducing the number of station time-series to 727.
- An additional pre-processing step consisted in weighing the observation anomalies by a given station's representative area (derived from a Delaunay triangulation iof station coordinates in a Transverse Mercator projection). The *weighted* dataset contains 727 station time-series, identical to the merged dataset.

The second subsection presents an in-depth analysis of the *degeneracy* of EOF computed from a gappy dataset, including North's rule-of-thumb (North et al., 1982; Hannachi et al., 2023; Storch and Zwiers, 1999) and its underlying estimate of the "effective sample size" (Thiébaux and Zwiers, 1984; Hannachi et al., 2007).

The third subsection presents *new results for the "gappy" EOF-based climate indicator* for temperatures across Sweden, and their comparison to previously submitted results. Overall, the corrected methodology yields similar results to the initial manuscript.

Both reviews strongly recommended a simplification of the manuscript's structure and content. For that purpose, several elements of the original study have been removed in the revised version:

- The dataset SMHI-ref (i.e. the climate indicator currently published by SMHI) was removed from the discussion. SMHI-ref is computed from 29 selected stations, from which individual station records are not available. This necessitated to compare the anomaly of the (spatially averaged) SMHI-ref climate indicator from its 1961–2018 mean (i.e. spatial prior to time averaging) to the spatial mean of 1961–2018 anomalies computed in the study (i.e. time prior to spatial averaging) – which added unnecessary confusion.

- Instead, a less ambiguous diagnostic was used: the difference between the EOF-based climate indicator and the arithmetic average for the same "gappy" dataset.

- In the original submission, the EOF computed on gap-filled observations were compared to MCA (maximum covariance analysis), erroneously referred to as SVD (singular value decomposition) between the same observations and the gridded GRIDCLIM dataset. Since this analysis does not provide a significant added value to the present study, all references to the SVD have been removed from the revised manuscript.

- The geographical interpretation of the EOF patterns is no longer part of the revised manuscript. While the EOF patterns and associated principal components presented in the original manuscript (Fig. (2–5) in Sturm (2024b)) are *per se* correct[1], they are no longer a priority in the revised version: since all datasets are consistently analysed for their spatial covariance $\widehat{\mathbf{S}} = \mathbf{X}^{\star}_{\text{ori}} \cdot {\mathbf{X}^{\star}_{\text{ori}}}^{\dagger}$, following Eq. (9), the new $\mathbf{EOF}$ are defined as a $n_{\text{time}} \times n_{\text{time}}$ square matrices, thus no longer suitable for a geographical interpretation.

- To demonstrate the new EOF computations from gappy datasets, only the annual mean (ANN) for temperature is shown here. Equivalent results for (annually-resolved) seasonal means (winter: DJF, spring: MAM, summer: JJA, autumn: SON) are also available; discussion of those results will be included in the revised manuscript.

- Suggestions for minor revisions, such as changes in formulation, typographic errors and figure labelling have not (yet) been considered at the present stage. Pending the reviewers' reaction to the major revisions presented in the revised version, the author will naturally incorporate all comments in the revised manuscript.

In conclusion, we are grateful to the didactic and encouraging remarks made by the reviewers. It allowed to revisit the fundamentals of EOF methodology (now summarised in the present appendix), and improve the quality of the manuscript by

[1] In the original manuscript, the centered observation matrix $\mathbf{X_c}$, of dimension $m_{\text{space}} \times n_{\text{time}}$, was centered around its time-mean: $\mathbf{X_c} = \mathbf{X} - \mu_{\text{time}}(\mathbf{X})$. Since the number of time-steps n_{time} is inferior to the number of station time-series m_{space} (i.e. $n_{\text{time}} < m_{\text{space}}$), the "economical" implementation of the EOF algorithm assumed a *de facto* spatial covariance analysis. This explains why the 1^{st} EOF pattern is unimodal, the 2^{nd} bi-modal etc.

incorporating the EOF computation on "gappy" datasets. Fortunately, this rigorous approach confirmed that the initial results (Sturm, 2024b) were correct, albeit not being sufficiently demonstrated.

This response to the reviews addresses primarily the requests for major revisions, from both a theoretical and numerical perspective. The sections hereafter also prefigure the structure and new graphs to be included in the revised manuscript version, pending to the new comments by reviewers. It is also worth mentioning that the methodological improvements described hereafter also apply to the 2nd companion article (Sturm, 2024a): the corresponding new graphs will be presented in the dedicated response to reviewers.

2 Demonstration of the original methodology

2.1 Gap-filling and centring of the MORA observation dataset

Let $\mathcal{X}(t,x)$ represent a climate variable (e.g. temperature) as a continuous function in time (noted t) and space (noted x). The $\mathcal{X}(t,xy)$ function is sampled at time-steps $t_i \in [[1, n_{\text{year}}]]$ and locations $x_j \in [[1, m_{\text{sta}}]]$; in other words, the function $\mathcal{X}(t,x)$ is discretised as a matrix $\mathbf{X}$, where:

$$\forall i \in [[1, n_{\text{year}}]], \forall j \in [[1, m_{\text{sta}}]], \mathbf{X_{i,j}} = \mathcal{X}(t_i, xy_j) \tag{1}$$

$\mathbf{X}$ is thus a matrix of dimensions $[n_{\text{year}}, m_{\text{sta}}]$, where each row $\forall i \in [[1, m_{\text{year}}]]$, $\mathbf{X}(i,:) = \overrightarrow{\mathcal{X}(t_i)}$ represents the spatial pattern at time-step t_i, and each column $\forall i \in [[1, n_{\text{sta}}]]$, $\mathbf{X}(:,j) = \overrightarrow{\mathcal{X}(xy_j)}$ the time-series at location x_j.

The present study focuses on annually resolved observation time-series, i.e. annual (ANN) or seasonal (DJF, MAM, JJA, SON) averages. Each annually resolved dataset is analysed independently, applying the procedure below.

Let $\mathbf{X}^{\star}_{\text{Full}}$ be the original MORA observation dataset over the entire study period 1860 – 2020, and $\mathbf{X}^{\star}_{\text{Cal}}$ its subset over the 1961–2018 calibration period. Both $\mathbf{X}^{\star}_{\text{Full}}$ and $\mathbf{X}^{\star}_{\text{Cal}}$ contain missing values, as indicated by th * symbol.

Let $\mathbf{X}^{\circ}_{\text{GridClim}}$ be a subset of the gridded GRIDCLIM dataset at the locations of $\mathbf{X}^{\star}_{\text{Cal}}$, applying nearest neighbour interpolation. GRIDCLIM dataset is complete (i.e. without missing values), as indicated by the $^{\circ}$ symbol.

Let $\mathcal{D} = \left[\overrightarrow{\mathcal{D}_1}, \ldots, \overrightarrow{\mathcal{D}_{n_{\text{year}}}}\right]^{\dagger}$ represent all non-missing values in observations in $\mathbf{X}^{\star}_{\text{Cal}}$, where $\overrightarrow{\mathcal{D}_1}$ represents all non-missing time-steps $t_i, \forall [[1, n_{\text{year}}$ at location xy_j. for and $\mathbf{X}^{\circ}_{\text{Cal}}$ the gap-filled MORA dataset. All matrices $\mathbf{X}^{\star}_{\text{Cal}}$, $\mathbf{X}^{\circ}_{\text{Cal}}$, $\mathbf{X}^{\circ}_{\text{GridClim}}$ share the same dimensions.

The for each location where $\mathbf{X}^{\star}_{\text{Cal}}$ displays missing values, a linear regression over the time-dimension is computed:

$$\text{Linear regression: } \forall i \in [[1, n_{\text{year}},]], \mathbf{X}^{\star}_{\text{Cal}}(i, j \in \overrightarrow{\mathcal{D}_i}) \approx a_i \cdot \mathbf{X}^{\circ}_{\text{GridClim}}(i, j \in \overrightarrow{\mathcal{D}_i}) + b_i$$

$$\Rightarrow \begin{cases} \mathbf{X}^{\circ}_{\text{Cal}}(i,j) = & \mathbf{X}^{\star}_{\text{Cal}}(i,j), & \forall (i,j) \in \mathcal{D} \\ \mathbf{X}^{\circ}_{\text{Cal}}(i,j) = & a_i \cdot \mathbf{X}^{\circ}_{\text{GridClim}}(i,j) + b_i, & \forall (i,j) \notin \mathcal{D} \end{cases} \tag{2}$$

Prior to performing the EOF analysis, the matrix $\mathbf{X} = \mathbf{X}^{\circ}_{\text{Cal}}$ needs to be centred, i.e. the temporal mean needs to be subtracted from each time-series. The centred matrix is noted $\mathbf{X_c}$ and defined in Eq. (3), where $\overrightarrow{\mu} = \mathcal{E}\left(\overrightarrow{X_j}\right), \forall j \in [[1, m_{\text{sta}}]]$ is a row vector of dimension $(1 \times m_{\text{sta}})$ representing the time-average (i.e. average along 1^{st} axis) of $\mathbf{X}^{\star}$ and $\overrightarrow{\mathbf{1}_{n_{\text{year}}}} = [1, \ldots, 1]^{\dagger}$ the n_{year}-dimension (column) unit-vector.

For the complete matrix $\mathbf{X}^{\circ}_{\text{Cal}}$, the time-average $\overrightarrow{\mu^{1961-2018}_{\text{time}}}$ can be computed explicitly. However, since $\mathbf{X}^{\circ}_{\text{GridClim}}$ is not defined outside the 1961–2018 calibration period, Eq. (2) cannot be applied to fill gaps. The $\overrightarrow{\widehat{\mu^{1860-2020}_{\text{time}}}}$ time-average for $\mathbf{X}^{\star}_{\text{Full}}$ is estimated solely based on available observation, i.e. $\forall (i,j) \in \mathcal{D}^{1860-2020}$.

$$
\begin{aligned}
\mathbf{X}^{\circ}_{\text{Cal}}, \forall t_i \in (1961, 2018) &\begin{cases} \forall j \in [[1, m_{\text{sta}}]], \mu(j) = \dfrac{1}{n_{\text{year}}} \cdot \displaystyle\sum_{i=1}^{n_{\text{year}}} x(i,j) \\ \qquad\qquad \Rightarrow x_c(i,j) = x(i,j) - \mu(j) \end{cases} \\
\mathbf{X}^{\star}_{\text{Full}}, \forall t_i \in (1860, 2020) &\begin{cases} \forall j \in [[1, m_{\text{sta}}]], \widehat{\mu(j)} = \dfrac{1}{|\overrightarrow{\mathcal{D}_i}|} \cdot \displaystyle\sum_{i \in \mathcal{D}_i} x^{\star}(i,j) \\ \qquad\qquad \Rightarrow x^{\star}_c(i,j) = x^{\star}(i,j) - \widehat{\mu(j)} \end{cases} \\
&\Leftrightarrow \mathbf{X^{\star}_c} = \mathbf{X}^{\star} - \overrightarrow{\mathbf{1}_{n_{\text{year}}}}^{\dagger} \cdot \widehat{\overrightarrow{\mu}}
\end{aligned} \tag{3}
$$

Given the significant differences in mean temperatures between southern and northern Sweden, it is preferable to reconstruct the national climate indicator based on anomalies rather than absolute observed values. When estimating the covariance matrix $\mathbf{S}$ of a "gappy" dataset, during which missing values are replaced by zeros (cf. Eq. (9)), anomalies introduce less bias than absolute values.

Absolute values can easily recovered by adding the mean $\widehat{\overrightarrow{\mu}}$ to anomalies $\mathbf{X} = \mathbf{X_c} + \overrightarrow{\mathbf{1}_{n_{\text{year}}}}^{\dagger} \cdot \widehat{\overrightarrow{\mu}}$.

2.2 Application to MORA reconstruction

This subsection investigates in more detail the methodology used in Sturm (2024b), in response to comments by (Anonymous, 2024a, b).

In this section, all observation datasets are assumed to be centred, i.e. $\mathbf{X} = \mathbf{X_c}$. This study focuses on the *spatial covariance*, we derive the n_{time} eigenvalues of covariance matrix $\mathbf{S'} = \mathbf{X} \cdot \mathbf{X}^{\dagger}$. According to Eq. (A7), $\mathbf{X}^{\circ}_{\text{cal}} = \mathbf{A}_{\text{cal}} \cdot {\mathbf{EOF}_{\text{cal}}}^{\dagger}$, where $\mathbf{A}$ is a n_{time} square matrix and $\mathbf{EOF}$ a unitary $[m_{\text{space}} \times n_{\text{time}}]$ matrix[2].

Let $(\boxtimes)^{\star}$ represent matrices with missing data, subscript $(\boxtimes)_{\text{cal}}$ refer to matrices defined over the calibration period 1961–2018, and $(\boxtimes)_{\text{rec}}$ to the full reconstruction period 1860–2020. Let $\widehat{(\boxtimes)}$ represent estimated variables obtained with a gappy dataset. Hence, $\mathbf{X}^{\star}_{\text{ori}}$ represents the original observations (with missing data), and $\widehat{\mathbf{X}_{\text{rec}}}$ the reconstructed dataset.

[2]According to Eq. (A13), the notations $\mathbf{EOF}$ and $\mathbf{A}$ can be considered as interchangeable. In the current case, EOF are defined as eigenvectors of the *spatial covariance*, the n_{time} eigenvector square matrix (transposed) is called $\mathbf{A}$, and the $[m_{\text{space}} \times n_{\text{time}}]$ (transposed) principal component matrix is called $\mathbf{EOF}$

In the present study, we assume *stationarity* for the EOF modes, therefore $\mathbf{EOF}_{\text{cal}} \equiv \widehat{\mathbf{EOF}_{\text{rec}}}$, with dimension $[m_{\text{space}} \times n_{\text{time}}]$. The principal components $\widehat{\mathbf{A}_{\text{rec}}}$ form a square matrix of rank n_{time}.

$$\widehat{\mathbf{A}_{\text{rec}}} = \mathbf{X}^{\star}_{\text{ori}} \cdot \mathbf{EOF}_{\text{cal}} \Rightarrow \widehat{\mathbf{X}_{\text{rec}}} = \widehat{\mathbf{A}_{\text{rec}}} \cdot \mathbf{EOF}_{\text{cal}}{}^{\dagger} \tag{4}$$

Let $\widehat{\mathbf{A}_{\text{rec}}}$ be the estimated matrix of principal components from 'gappy' data $\mathbf{X}^{\star}_{\text{ori}}$. Let n_{time} be the number of eigenvalues for the covariance matrix $\mathbf{S}$. Since $n_{\text{year}} < m_{\text{sta}}$, $n_{\text{time}} = n_{\text{year}}$ for the full EOF decomposition. Let $\mathcal{D} = \left[\overrightarrow{\mathcal{D}_1}, \ldots, \overrightarrow{\mathcal{D}_{n_{\text{year}}}}\right]^{\dagger}$ represent all non-missing values in $\mathbf{X}^{\star}_{\text{ori}}$ and $\mathcal{N} = \left[\overrightarrow{\mathcal{N}_1}, \ldots, \overrightarrow{\mathcal{N}_{n_{\text{year}}}}\right]^{\dagger}$ all missing values.

Let $\overrightarrow{e_{i,\star}}\Big|_{j \in \overrightarrow{\mathcal{D}_i}}$ represent the eigenvector $\overrightarrow{e_i}$ at locations where $\mathbf{X}^{\star}_{\text{ori}}$ is defined.

$$\begin{aligned}
\overrightarrow{e_{i,\star}}\Big|_{j \in \overrightarrow{\mathcal{D}_i}} &= \begin{cases} e_{i,j} \forall j \in \overrightarrow{\mathcal{D}_i} \\ 0 \text{ otherwise} \end{cases} \Leftrightarrow \overrightarrow{e_i} = \overrightarrow{e_{i,\star}}\Big|_{j \in \overrightarrow{\mathcal{D}_i}} + \overrightarrow{e_{i,\star}}\Big|_{j \notin \overrightarrow{\mathcal{D}_i}} \\
\Leftrightarrow \langle \overrightarrow{e_i}, \overrightarrow{e_k} \rangle &= \langle \overrightarrow{e_{i,\star}}\Big|_{j \in \overrightarrow{\mathcal{D}_i}}, \overrightarrow{e_k} \rangle + \langle \overrightarrow{e_{i,\star}}\Big|_{j \notin \overrightarrow{\mathcal{D}_i}}, \overrightarrow{e_k} \rangle \\
\Leftrightarrow \langle \overrightarrow{e_{i,\star}}\Big|_{j \in \overrightarrow{\mathcal{D}_i}}, \overrightarrow{e_k} \rangle &= \delta_{i,j} - \langle \overrightarrow{e_{i,\star}}\Big|_{j \notin \overrightarrow{\mathcal{D}_i}}, \overrightarrow{e_k} \rangle
\end{aligned} \tag{5}$$

Eq. (5) demonstrates that the presence of missing values in $\mathbf{X}^{\star}_{\text{ori}}$ that "gappy" eigenvectors are no longer mutually orthogonal: $\langle \overrightarrow{e_{i,\star}}\Big|_{j \notin \overrightarrow{\mathcal{D}_i}}, \overrightarrow{e_k} \rangle \neq \delta_{i,k}$. Bearing this in mind, the first step in the field reconstruction is to project $\mathbf{X}^{\star}_{\text{ori}}$ onto the $\mathbf{EOF}_{\text{cal}}$ eigenvectors calculated during the 1961–2018 calibration period, as shown in Eq. (6).

$$\begin{aligned}
\widehat{\alpha_{i,k}} &= \mathcal{E}\left(\langle \overrightarrow{x^{\star}_i}, \overrightarrow{e_k} \rangle\right) = \frac{1}{|\overrightarrow{\mathcal{D}_i}|} \cdot \sum_{l \in \overrightarrow{\mathcal{D}_i}} x^{\star}_{i,l} \cdot e_{l,k} = \frac{1}{|\overrightarrow{\mathcal{D}_i}|} \cdot \left(\widehat{\mathbf{X}^{\star}_{\text{ori}}} \cdot \overrightarrow{e_{k,\star}}\Big|_{l \in \overrightarrow{\mathcal{D}_k}}\right) \\
\Leftrightarrow \widehat{\overrightarrow{\alpha_i}} &= \frac{1}{|\overrightarrow{\mathcal{D}_i}|} \cdot \sum_{k=1}^{n_{\text{time}}} \widehat{\mathbf{X}^{\star}_{\text{ori}}} \cdot \overrightarrow{e_{k,\star}}\Big|_{l \in \overrightarrow{\mathcal{D}_k}}
\end{aligned} \tag{6}$$

Eq. (A8) demonstrates that principal components $\overrightarrow{\alpha_i}$ are mutually orthogonal. As a corollary to Eq. (5), the *estimated* principal components $\widehat{\overrightarrow{\alpha_i}}$ are no longer orthogonal to each other (i.e. $\langle \widehat{\overrightarrow{\alpha_i}}, \widehat{\overrightarrow{\alpha_k}} \rangle \neq \delta_{i,k} \cdot \lambda_k$). This particularity was pointed out in anonymous reviews (Anonymous, 2024a, b).

$$\begin{aligned}
\widehat{x_{i,j}} &= \sum_{k=1}^{n_{\text{time}}} \widehat{\alpha_{i,k}} \cdot e_{k,j} = \langle \widehat{\overrightarrow{\alpha_i}}, \overrightarrow{e_j}^{\dagger} \rangle = \frac{1}{|\overrightarrow{\mathcal{D}_i}|} \cdot \sum_{k=1}^{n_{\text{time}}} \left(\sum_{l \in \overrightarrow{\mathcal{D}_i}} x^{\star}_{i,l} \cdot e^{\star}_{l,k} \right) \cdot e_{k,j} \\
\Leftrightarrow \widehat{\overrightarrow{x_i}} &= \frac{1}{|\overrightarrow{\mathcal{D}_i}|} \cdot \sum_{j=1}^{n_{\text{time}}} \left(\widehat{\mathbf{X}^{\star}_{\text{ori}}} \cdot \overrightarrow{e_{i,\star}}\Big|_{k \in \overrightarrow{\mathcal{D}_i}} \right) \cdot \overrightarrow{e_j}^{\dagger}
\end{aligned} \tag{7}$$

Eq. (7) illustrates the method described in Sturm (2024b, a). We can thus conclude that the estimated climate indicator $\widehat{CI_{\text{rec}}}|_{t=t_i}) = \mathcal{E}\left(\widehat{\overrightarrow{x_i}}\right)$ is indeed different from $\widehat{CI_{\text{ori}}}|_{t=t_i}) = \mathcal{E}\left(\overrightarrow{x^{\star}_i}\right)$.

Without a priori knowledge of the structure of $\overrightarrow{\mathcal{D}_i}$, thus $\overrightarrow{e_{i,\star}}$ and $\widehat{\overrightarrow{\alpha_i}}$, no analytical solution can be derived for $\langle\widehat{\overrightarrow{\alpha_i}}, \widehat{\overrightarrow{\alpha_k}}\rangle$. The following subsection explores the numerical assessment for this case study.

2.3 Estimation of the mean climate indicator

The climate indicator $\widehat{\overrightarrow{CI}}$, computed as the mean of all values for a given time-step, can be expressed as the expectation $\mathcal{E}$ of the matrix $\mathbf{X} = (\overrightarrow{x}_1, \ldots, \overrightarrow{x}_{m_{\text{sta}}})$.

Let $|D_i| \leq m_{\text{sta}}$ represent the number of available observations at time-step t_i in $\overrightarrow{x}_i = \mathbf{X}_i = \mathbf{X}(i,:)$. Let $\overrightarrow{e_i} = \mathbf{EOF}_{\text{cal}}|_{t=t_i}$ be the eigenvector corresponding to the i^{th} eigenvalue, where $i \in [[1, n_{\text{time}}]]$.

The climate indicator $\widehat{\overrightarrow{CI_{\text{rec}}}}$ can thus be estimated as an arithmetic mean of non-missing values:

$$\begin{aligned}
\widehat{CI_{\text{rec}}}|_{t=t_i} &= \mathcal{E}\left(\widehat{\overrightarrow{x_i}}\right) = \mathcal{E}\left(\frac{1}{|\overrightarrow{\mathcal{D}_i}|} \cdot \sum_{j=1}^{n_{\text{EOF}}} \left(\widehat{\mathbf{X}^{\star}_{\text{ori}}} \cdot \overrightarrow{e_{i,\star}}\Big|_{k\in\overrightarrow{\mathcal{D}_i}}\right) \cdot \overrightarrow{e_j}^{\dagger}\right) \\
\Leftrightarrow \widehat{CI_{\text{rec}}}|_{t=t_i} &= \frac{\left(\mathbf{X}^{\star}_{\text{ori}} \cdot \overrightarrow{e_{i,\star}}\Big|_{k\in\overrightarrow{\mathcal{D}_i}}\right) \cdot \overrightarrow{e_i}^{\dagger}}{|\overrightarrow{\mathcal{D}_i}|}
\end{aligned} \tag{8}$$

Eq. (8) hence provides a formal demonstration for Eq. (6) in Sturm (2024b).

3 Extension of the methodology to gappy datasets

3.1 Estimation of the covariance of a dataset with missing values

The first review (Anonymous, 2024a) accurately emphasises that EOF can be computed from datasets with missing values, e.g. demonstrated by Storch and Zwiers (1999)'s section on "gappy" datasets. This possibility, overseen in the first version of the manuscript, allows to apply the method on the full observation dataset (hereafter referred to as CI-full, analogously to CI-cal for the calibration network).

Following Storch and Zwiers (1999), the covariance matrix $\widehat{\mathbf{S}} = \left[\ddots, \widehat{\sigma_{i,j}}, \ddots\right]$, a square matrix with elements noted $\widehat{\sigma_{i,j}}$ can be estimated as following:

$$\begin{aligned}
\widehat{\sigma_{i,j}} &= \frac{1}{|K_i \cap K_j|} \sum_{k\in K_i\cap K_j} (x_{k,i} - \widehat{\mu_i}) \cdot (x_{k,j} - \widehat{\mu_j})^* \\
\text{where } \widehat{\mu_i} &= \frac{1}{|K_i|} \sum_{k\in K_i} x_{k,i}
\end{aligned} \tag{9}$$

To avoid missing values in $\widehat{\mathbf{S}}$, Eq. (9) needs to apply to the *spatial covariance* of the MORA observations; according to Eq. (A12), it implies that $\widehat{\mathbf{S}}$ is a n_{time} square matrix. Following Eq. (A5) and Eq. (A7), we can estimate the reconstructed dataset $\widehat{\mathbf{X}_{\text{rec}}}$ following Eq. (10).

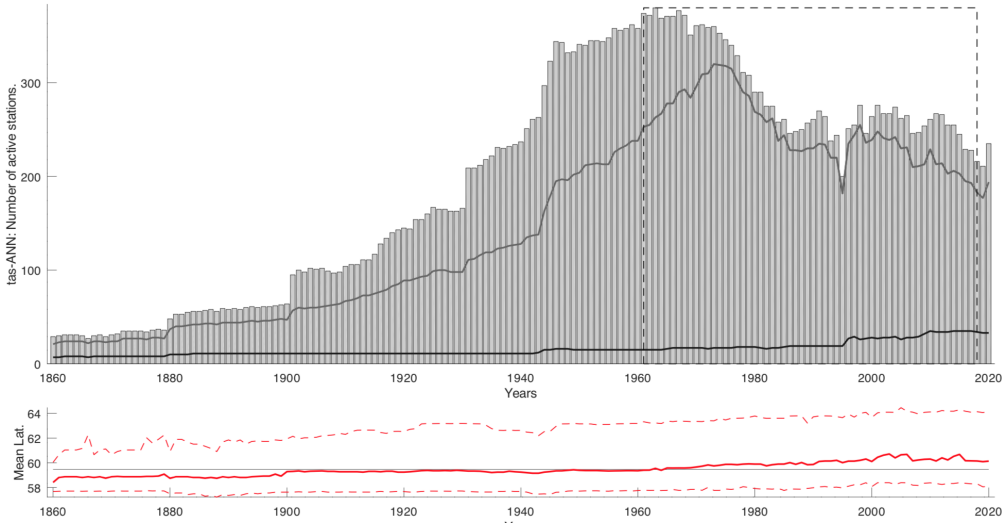

Figure 1. Upper plot: Number of active temperature stations in MORA over time (as bars). The dark grey line represents the number of active in the original reference station network; they light grey line represents the number of stations for the calibration network (i.e. individual stations being active at least 15 years during the calibration period 1961–2018, as highlighted by the dashed box). Lower plot: Median latitude for active stations in the calibration data-set over time (incl. the $[25\%\tilde{}75\%]$ bounds). The median latitude is used as a proxy for the distribution of the observation network. (This figure is reproduced from the original manuscript (Sturm, 2024b).)

$$\widehat{\mathbf{S}} \cdot \widehat{\mathbf{EOF}} = \widehat{\mathbf{EOF}} \cdot \widehat{\Lambda} \Leftrightarrow \widehat{\mathbf{S}} = \widehat{\mathbf{EOF}} \cdot \widehat{\Lambda} \cdot \widehat{\mathbf{EOF}}^{\dagger} \tag{10}$$
$$\Rightarrow \widehat{\mathbf{X}_{\text{rec}}} = \langle \mathbf{X}^{\star}_{\text{ori}}, \widehat{\mathbf{EOF}} \rangle \cdot \widehat{\mathbf{EOF}}^{\dagger}$$

The second review (Anonymous, 2024b) raises the question of the geometry of the observation network, and whether missing values are randomly distributed. This is indeed a crucial aspect, which is not thoroughly covered in the original manuscript.

To answer this question, additional preprocessing steps need to be applied to the observational datasets. In the original manuscript (Fig. (1) and Table (1) in Sturm (2024b)), the *total network*, i.e. 993 time-series of *temperature* observations, were reduced to 466 time-series for the *calibration network*. In order to qualify for the calibration network, a given station has to (i) have at least 15 years of data coverage during the 1961–2018 calibration period, and (ii) a correlation coefficient (for annually resolved records) $r > \sqrt{0.5}$ with the nearest-neighbour grid-cell in the GRIDCLIM dataset. Isolating a suitable calibration network is required, in the original method, in order to construct a complete (i.e. NaN-free) MORA dataset prior to computing EOF over the 1961–2018 calibration period.

Thus emerges a new issue with the CI-full network geometry: the MORA database contains stations with nearly identical geographical coordinates, but active over different time-periods (generally with a few year overlap). It is therefore usual to construct time-series with fewer missing values by "stitching" (aka. as coupling or merging) neighbouring stations into a single record (Sturm, 2024b; Joelsson et al., 2023).

In the present document, an automatic merging was performed by merging stations located in a 5 km radius: the synthetic time-series is taken as the mean of available (i.e. arithmetic average, for each time-step, disregarding NaN). As a result, the *merged network* is reduced from 993 to 727 time-series: this operation avoids duplicate time-series with long periods of missing values. However, the merging procedure does not explicitly addresses the station density. It is obvious from Fig. (1, lower panel: median latitude of active stations over time) and Fig. (2) in Sturm (2024b) that more observation stations are operated in the South (more populated) regions of Sweden (especially prior to 1900). Hence EOF are also computed after weighing each time-series' anomaly by the station's representative area (obtained by Delaunay triangulation of the station's coordinate in the Rikets Nät 1990 (RT90)/Transverse Mercator projection). The *weighted network* has by construction the same number of station time series (727) as the merged network. The relevance of spatial weighted anomalies for EOF analyses of climate observations is documented e.g. in North et al. (1982); Quayle et al. (1991); Thomson and Emery (2014); Zhang and Moore (2015).

3.2 Degeneracy of gappy EOF computations

The eigenvalues $\widehat{\lambda}$ computed from the GRIDCLIM and MORA datasets are shown in Fig. (2), and corresponding values in Table (1). $\widehat{\lambda}$ FOR GridClim-sub are presented with all available preprocessing (*original*, i.e. 993 grid-cells), and the *merged* and *weighted* processed (727) over the 1961–2018 calibration period. Similarly MORA-full-F represents the $\widehat{\lambda}$ for the full (original), merged and weighted datasets over the entire study period (1860–2020). MORA-cal-N represents the gap-filled observation dataset for the calibration network (466 stations) over 1961–2018, as described in (Sturm, 2024b). For comparison purposes, MORA-short-X represents a subset of the 1860–2020 MORA-full-F dataset, sampled at the same locations as MORA-cal-N (i.e. the calibration network).

Unsurprisingly, we notice that datasets without missing values (i.e. GridClim-sub and MORA-cal-N) display an effective sample size (n'_{EOF}) identical to $\mathbf{S}$'s rank: n_{time}. Accordingly, the non-degenerate EOF account for almost all of $\mathbf{X}$'s variance ($\sum \widehat{\lambda} > 97\%$). Among datasets with missing values, MORA-short-X, i.e. a subset of MORA-full-F, restricted to the calibration network, displays a slightly higher percentage of the variance ($\sum \lambda = 76\%$) compared to MORA-full-F ($\sum \lambda = 64\%$).

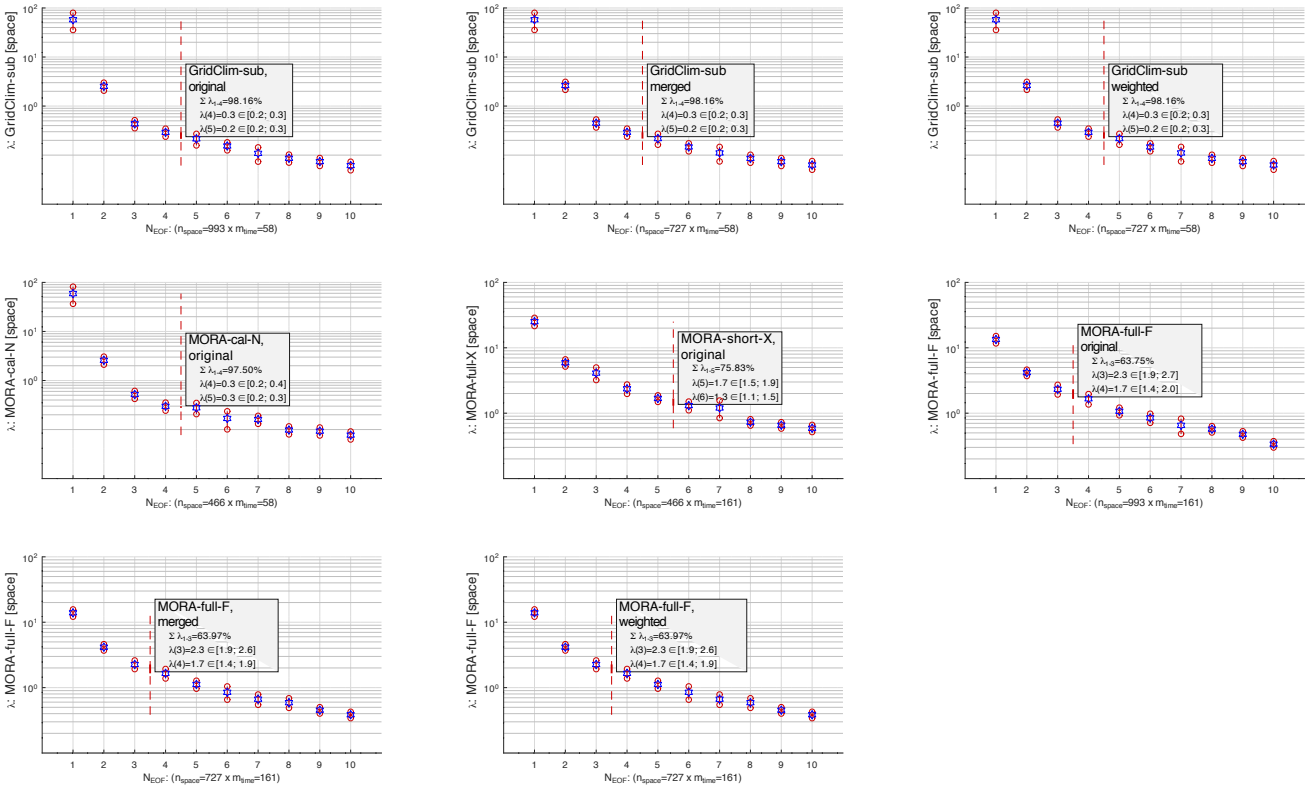

Figure 2. Eigenvalue ($\widehat{\lambda}$) plots for the GRIDCLIM and MORA datasets, in original, merged and weighted form. MORA-cal-N represents the gap-filled observation dataset for the calibration network (466 stations) over 1961–2018. MORA-short-X represents a subset of MORA-full-F dataset, sampled at the same locations as MORA-cal-N. Corresponding values for EOF degeneracy are shown in Table (1). The dashed vertical line indicates the first degenerate λ. The Y-axis shows λ on a logarithmic scale.

Dataset	**Description**	N_{dim}	$n'_{\text{EOF/tot}}$	$N_{\text{EOF-degn}}$	$\sum_{k=1}^{\lambda_{N^{\text{EOF-degn}}}}$	$\lambda_{N^{\text{EOF-degn}}}$	$\lambda_{N^{\text{EOF-degn}}+1}$
GridClim-sub: ori	Temperature obs. for ANN, GRIDCLIM, 1961-2018 calibration period, original	993×58	$58/58$	$[4, 7]$	98.16%	$\lambda_4 = 0.3 \in [0.2; 0.3]$	$\lambda_5 = 0.2 \in [0.2; 0.3]$
GridClim-sub: mrg	Temperature obs. for ANN, GRIDCLIM, 1961-2018 calibration period, merged	727×58	$58/58$	$[4, 7]$	98.16%	$\lambda_4 = 0.3 \in [0.2; 0.3]$	$\lambda_5 = 0.2 \in [0.2; 0.3]$
GridClim-sub: wgt	Temperature obs. for ANN, GRIDCLIM, 1961-2018 calibration period, weighted	727×58	$58/58$	$[4, 7]$	98.16%	$\lambda_4 = 0.3 \in [0.2; 0.3]$	$\lambda_5 = 0.2 \in [0.2; 0.3]$
MORA-cal: N, ori	Temperature obs. for ANN, MORA, 1961-2018 calibration period, after gap-filling, original	466×58	$58/58$	$[4, 4]$	97.50%	$\lambda_4 = 0.3 \in [0.2; 0.4]$	$\lambda_5 = 0.3 \in [0.2; 0.3]$
MORA-short: X, ori	Temperature obs. for ANN, MORA, 1860-2020 full study period, with missing values, original	466×161	$152/161$	$[5, 6]$	75.83%	$\lambda_5 = 1.7 \in [1.5; 1.9]$	$\lambda_6 = 1.3 \in [1.1; 1.5]$
MORA-full: F, ori	Temperature obs. for ANN, MORA, 1860-2020 full study period, with missing values, original	993×161	$70/161$	$[3, 7]$	63.75%	$\lambda_3 = 2.3 \in [1.9; 2.7]$	$\lambda_4 = 1.7 \in [1.4; 2.0]$
MORA-full: F, mrg	Temperature obs. for ANN, MORA, 1860-2020 full study period, with missing values, merged	727×161	$88/161$	$[3, 6]$	63.97%	$\lambda_3 = 2.3 \in [1.9; 2.6]$	$\lambda_4 = 1.7 \in [1.4; 1.9]$
MORA-full: F, wgt	Temperature obs. for ANN, MORA, 1860-2020 full study period, with missing values, weighted	727×161	$88/161$	$[3, 6]$	63.97%	$\lambda_3 = 2.3 \in [1.9; 2.6]$	$\lambda_4 = 1.7 \in [1.4; 1.9]$

Table 1. Parameters describing the EOF degeneracy. N_{dim} indicates the dimensions of the $\mathbf{X}$ dataset. $n'_{\text{eff/tot}}$ represents the effective sample size (Eq. (A17), (Thiébaux and Zwiers, 1984)), compared to the (total) $\mathbf{S}$ rank (i.e. n_{time} for the spatial covariance matrix $\mathbf{S}$, Eq. (A12)). $N_{\text{EOF-degn}}$ represents the highest non-degenerate EOF rank: the first bracket element represents the $N_{\text{EOF-degn}}$ estimate according to North's rule-of-thumb Eq. (A18), the second according to the Kaiser rule (Eq. (A14), (Wilks, 2006)). $\sum_{k=1}^{\lambda_{N^{\text{EOF-degn}}}}$ represents the percentage of explained variance of non-degenerate EOF. $\lambda_{N^{\text{EOF-degn}}}$ and $\lambda_{N^{\text{EOF-degn}}+1}$ represent the eigenvalue with its 95% confidence interval (Eq. (A19), (Hannachi et al., 2007)).

3.3 Reconstruction of the climate indicator from gappy EOF

The climate indicator $\widehat{\overrightarrow{CI}}$ for temperature can be reconstructed using Eq. (11), where $\mathcal{D}_i$ represents all non-missing values in the original dataset $\mathbf{X}^{\star}_{\text{ori}}$ at the time-step $t = t_i$, $\widehat{\overrightarrow{CI}_{\text{AM}}}$ the original (i.e. arithmetic mean) climate indicator and $\widehat{\overrightarrow{CI}_{\text{EOF}}}$ the EOF-based climate indicator. It is worth noting that Eq. (11) is valid regardless of the scaling convention of $\widehat{\mathbf{EOF}_{\text{cal}}}$.

$$\widehat{\overrightarrow{CI}_{\text{CM}}} = \sum_{j \in \mathcal{D}_i} \frac{1}{|\mathcal{D}_i|} \cdot \mathbf{X}^{\star}_{\text{ori}}$$
$$\widehat{\overrightarrow{CI}_{\text{EOF}}} = \frac{1}{m_{\text{space}}} \cdot \sum_{j=1}^{m_{\text{space}}} \widehat{\mathbf{A}} \cdot \widehat{\mathbf{EOF}}^{\dagger} = \frac{1}{m_{\text{space}}} \cdot \sum_{j=1}^{m_{\text{space}}} \langle \mathbf{X}^{\star}_{\text{ori}}, \widehat{\mathbf{EOF}} \rangle \cdot \widehat{\mathbf{EOF}}^{\dagger} \tag{11}$$

For all datasets in Table (1), $\widehat{\mathbf{EOF}}$ is computed from gappy datasets according to Eq. (10) . Note that $\mathbf{X}^{\star}_{\text{ori}}$ in Eq. (11) can represent the *full* (original), *merged* or *weighted* station network, with their respective $\widehat{\mathbf{EOF}}$. For datasets noted as "MORA-cal X MORA-full" and "GridClim-full X MORA-full" in Fig. (3) and Fig. (4), $\widehat{\overrightarrow{CI}_{\text{EOF}}}$ is computed by projecting $\mathbf{X}^{\star}_{\text{ori}}$ on $\widehat{\mathbf{EOF}}$ computed over the 1961–2018 calibration period (i.e. the square matrices $\widehat{\mathbf{EOF}}$, of dimension $2018 - 1961 + 1 = 58$, for MORA-cal and GridClim-full), analogously to Eq. (8) and Sturm (2024b).

Fig. (3) shows the estimated climate indicator $\widehat{\overrightarrow{CI}}$ in *absolute* values (i.e. mean temperature over Sweden in °C). By construction, the estimated climate indicator from original (arithmetic) $\widehat{\overrightarrow{CI}_{\text{AM}}}$ and the EOF-based $\widehat{\overrightarrow{CI}_{\text{EOF}}}$ are identical for datasets without any missing values (i.e. GridClim-full and MORA-cal). GridClim-full is presented in Fig. (3) with 3 preprocessing: the *original* (i.e. 993 station time-series), the *merged* and *weighted* versions (727). The comparison over the 1961–2018 calibration period indicates that all 3 version are highly correlated, with $\widehat{\overrightarrow{CI}_{\text{original}}} > \widehat{\overrightarrow{CI}_{\text{merged}}} > \widehat{\overrightarrow{CI}_{\text{weighted}}}$. This is consistent with the fact that that observations in southern Sweden, characterised by higher temperatures, (i) are more abundant in early parts of the record (therefore more likely to present more neighbour stations to be merged, hence $\widehat{\overrightarrow{CI}_{\text{original}}} > \widehat{\overrightarrow{CI}_{\text{merged}}}$); (ii) present a higher station density than in Sweden's northern parts (as demonstrated by the median and $[25\%, 75\%]$ percentiles of the station's latitude (Sturm, 2024b), Fig. (1)), hence $\widehat{\overrightarrow{CI}_{\text{merged}}} > \widehat{\overrightarrow{CI}_{\text{weighted}}}$. In summary, the $\widehat{\overrightarrow{CI}_{\text{original}}}$, $\widehat{\overrightarrow{CI}_{\text{merged}}}$, $\widehat{\overrightarrow{CI}_{\text{weighted}}}$ display a close variability with an ~ 0.1°C offset for the Sweden average.

Over the 1860–2020 study period, all estimated climate indicators $\widehat{\overrightarrow{CI}}$ display a similar inter-annual variability, with increasingly negative offset for $\widehat{\overrightarrow{CI}_{\text{EOF}}}$ (full lines) versus $\widehat{\overrightarrow{CI}_{\text{ori}}}$ (dashed lines) prior to 1930. In order to better assess the difference between $\widehat{\overrightarrow{CI}_{\text{EOF}}}$ and $\widehat{\overrightarrow{CI}_{\text{ori}}}$, Fig. (4) represents $\Delta\widehat{\overrightarrow{CI}} = \widehat{\overrightarrow{CI}_{\text{EOF}}} - \widehat{\overrightarrow{CI}_{\text{ori}}}$, i.e. the subtraction of full ($\widehat{\overrightarrow{CI}_{\text{EOF}}}$) and dashed ($\widehat{\overrightarrow{CI}_{\text{ori}}}$) lines in Fig. (3).

Fig. (4) demonstrates the equivalent results between the $\mathbf{EOF}_{\text{cal}}$, i.e. the gap-filled $\mathbf{X}^{\circ}$ over the 1961–2018 period (based on the 466-station calibration network), and the "gappy" $\widehat{\mathbf{EOF}}$, computed from Eq. (10) (cf. dataset definitions in Table (1)):

- MORA-cal X MORA-full is virtually identical to MORA-short: $\widehat{\mathbf{EOF}_{\text{MORA-short}}}$, computed from the (gappy) subset at the 466 stations of the 1860–2020 $\mathbf{X}^{\star}_{\text{ori}}$ dataset, is thus equivalent to $\mathbf{EOF}_{\text{cal}}$ computed from the 1961–2018 gap-filled $\mathbf{X}^{\circ}_{\text{MORA}}$ dataset in Eq. (2).

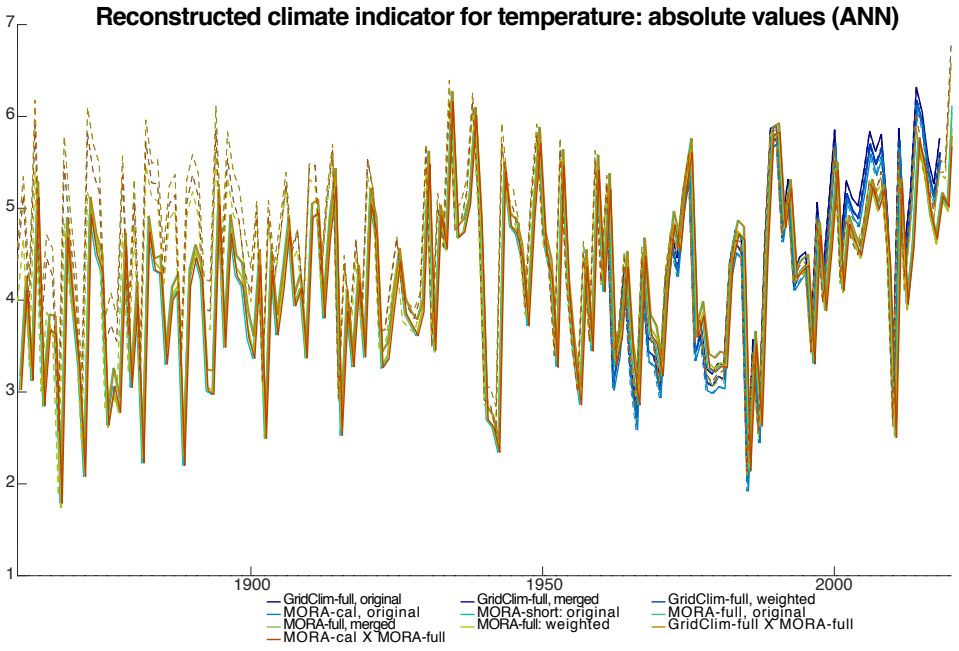

Figure 3. Reconstructed climate indicator for temperature for annual means (ANN). The legend shows the dataset (MORA or GRIDCLIM) and preprocessing (original, merged or weighted) as defined in Table (1). Full lines represent $\widehat{\overrightarrow{CI}}_{\text{EOF}}$, the EOF-reconstructed climate indicator; dashed lines the $\widehat{\overrightarrow{CI}}_{\text{AM}}$ reference (i.e. arithmetic mean, for a given time-step, over all available station observations for a given dataset).

– GridClim-full X MORA-full is virtually identical to MORA-full: $\widehat{\mathbf{EOF}}_{\text{MORA-full}}$, computed from the total 933-station (gappy) $\mathbf{X}^{\star}_{\text{ori}}$, is thus equivalent to $\mathbf{EOF}_{\text{GridClim-full}}$, the subset of the (complete) gridded GRIDCLIM sampled at the 993-station MORA locations.

This result confirms the comment for major revision by Anonymous (2024a)[3]: while the method originally described in Sturm (2024b) fails to enforce the orthogonality for the projection of the gappy dataset, its result is equivalent to the rigorous EOF-computation following Storch and Zwiers (1999)'s section on "gappy" datasets. It furthermore demonstrates that the spatial covariance ($\mathbf{S} = \mathbf{X} \cdot \mathbf{X}^{\dagger}$) of the 1961–2018 GRIDCLIM (sampled at the MORA 933-station locations) is equivalent to $\widehat{\mathbf{S}_{\text{MORA-full}}}$, computed with Eq. (9) from the gappy 1860-2020 MORA dataset.

The corrected method reinforces the initial conclusion in Sturm (2024b): the difference $\Delta\widehat{\overrightarrow{CI}}$ between the reference (arithmetic averaged) $\widehat{\overrightarrow{CI}}_{\text{ori}}$ and the EOF-based $\widehat{\overrightarrow{CI}}_{\text{EOF}}$ reconstructed climate indicator amounts to ~ -1°C over the 1880–1900 period for the *full* and *merged* versions gappy $\mathbf{X}^{\star}_{\text{ori}}$ dataset. In other words, compute the climate indicator for temperatures over Sweden as the arithmetic mean of available observations introduces a significant positive bias for the period prior to 1930. This

[3] "Perhaps more importantly, the EOF-based method contains some technical errors that need to be addressed, although I believe these changes would not strongly impact the final results."

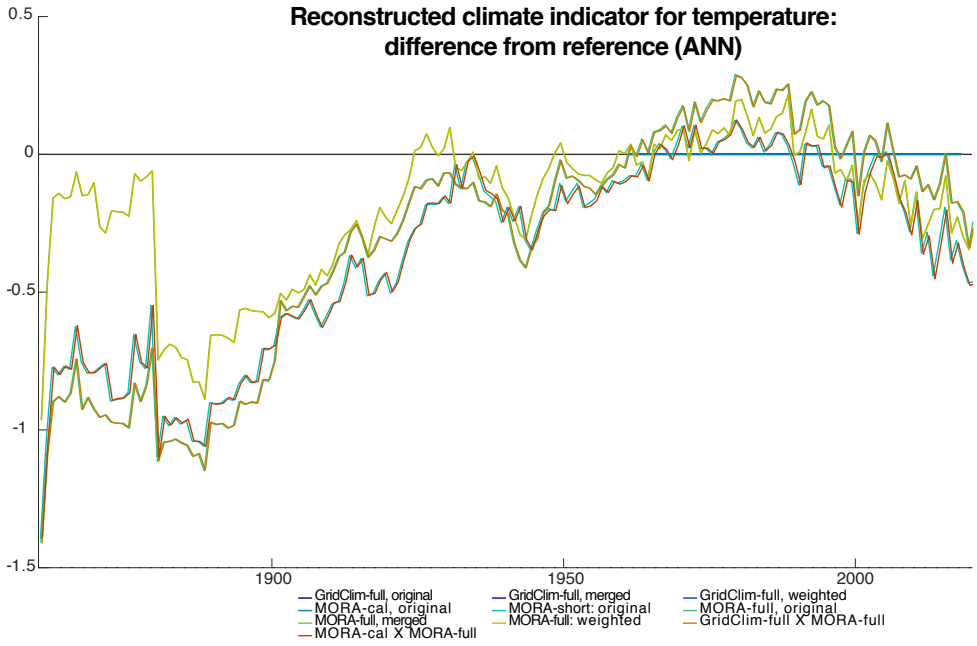

Figure 4. Difference between the reconstructed climate indicator and the reference method, for temperature for annual means (ANN). The legend shows the dataset (MORA or GRIDCLIM) and preprocessing (original, merged or weighted) as defined in Table (1). In other words, lines represent the $\Delta\widehat{\overrightarrow{CI}} = \widehat{\overrightarrow{CI}}_{\mathrm{EOF}} - \widehat{\overrightarrow{CI}}_{\mathrm{ori}}$, subtraction of full and dashed lines in Fig. (3). The slight offset in time (X) coordinates for various datasets is a plotting artefact to distinguish similar curves: all refer to the same date.

bias is primarily due to the fact that observations in Sweden's southern (warmer) regions are more abundant prior to 1900, as shown in the spread of latitude of active stations over time (Fig. (1) in Sturm (2024b)).

Following the reviewers' suggestion, we introduce a new, *weighted* climate indicator: the observed station anomaly is weighted by the a given station's representative area (based on Delaunay triangulation of station coordinates in a Transverse Mercator projection). Stations in the less densely sampled northern regions thus gain a larger influence on the aggregated national climate indicator. The *weighted* EOF-based climate indicator displays a negative bias compared to the *reference* (i.e. arithmetically averaged) indicator as well, albeit of lesser amplitude ($\Delta\widehat{\overrightarrow{CI}} \sim -0.75°\mathrm{C}$ for the 1880–1900 mean). The weighed climate indicator however does not appear robust prior to 1880, as a result of the scarcity of observations in northern Sweden in early records.

4 Conclusions

Comments and suggestions for major revisions by Anonymous (2024a, b) allowed a significant improvement of the original manuscript (Sturm, 2024b): the author is deeply grateful to the reviewers' efforts. The major improvements are listed hereafter:

– The fundamentals of EOF calculus, in particular the impact of $time \times space$ versus $space \times time$ convention for the dimension of the $\mathbf{X}^{\star}_{\text{ori}}$ observation matrix, was reviewed with help of suggested bibliography references (Hannachi et al., 2023, 2007; Storch and Zwiers, 1999; Björnsson and Venegas, 1997; Preisendorfer, 1988). The summary, with consistent notation, is presented in the appendix.

– The possibility to compute EOF (wrt. $\mathbf{X}^{\star}_{\text{ori}}$ *spatial covariance*) from "gappy" datasets (i.e. with missing values) was explored from both an analytical and numerical perspective. As a corollary, this study investigates the EOF *degeneracy* with North's rule-of-thumb (North et al., 1982; Hannachi et al., 2023; Storch and Zwiers, 1999) and its underlying estimate of the "effective sample size" (Thiébaux and Zwiers, 1984; Hannachi et al., 2007).

– To investigate the impact the distribution of missing values in space and time in the observation matrix $\mathbf{X}^{\star}_{\text{ori}}$, we define 3 preprocessing options: the *original*, full (993 station time-series) dataset; the *merged* dataset, where neighbouring stations (within a 5-km radius) are averaged to a synthetic time-series with lesser missing values; the *weighted* dataset, where observed anomalies of merged time-series are weighted by each station's representative area (obtained by Delaunay triangulation of the station's coordinate in the Rikets Nät 1990 (RT90)/Transverse Mercator projection).

The methodological improvements above lead to new findings, which reinforce the conclusions of the initial study. The EOF-based climate indicator for temperatures in Sweden $\widehat{\overrightarrow{CI}_{\text{EOF}}}$, shown in Fig. (3) and Fig. (4) is inferior to the arithmetical mean of available observations $\widehat{\overrightarrow{CI}_{\text{AM}}}$ by up to $-1°\text{C}$ prior to 1900, when all station time-series in $\mathbf{X}^{\star}_{\text{ori}}$ are considered individually (*original* preprocessing) or neighbouring stations are merged into synthetic time-series (*merged* preprocessing). The difference is reduced to $-0.75°\text{C}$ if anomalies in $\mathbf{X}^{\star}_{\text{ori}}$ are weighted by the station's representative area (*weighted* preprocessing). This result is related to the particular "shape" of the Swedish observation network. Stations in the southern parts generally extend further back in time (with a higher nummer of duplicate/neighbouring stations), with a higher spatial density than in their northern counterparts; for obvious climatological reasons, southern Sweden is characterised by higher mean annual temperatures.

The use of the diagnostic $\Delta\widehat{\overrightarrow{CI}} = \widehat{\overrightarrow{CI}_{\text{EOF}}} - \widehat{\overrightarrow{CI}_{\text{ori}}}$, computed for various datasets (i.e. subsets of MORA and GRIDCLIM) and preprocessing (i.e. *original*, *merged* and *weighted*) is convenient to assess the bias of station location and data availability on a national climate indicator for temperature in Sweden: the EOF-based $\widehat{\overrightarrow{CI}_{\text{EOF}}}$ proves less sensitive than the arithmetic mean $\widehat{\overrightarrow{CI}_{\text{AM}}}$ to the distribution of missing values in $\mathbf{X}^{\star}_{\text{ori}}$. This result can be further investigated using Monte-Carlo and/or sensitivity to white-noise perturbations (Sturm, 2024b).

The investigation of EOF from gappy datasets further strengthens the validity of the methodology presented in Sturm (2024b) (despite its lack of formal demonstration): reconstruction of the principal component matrix $\widehat{\mathbf{X}_{\text{rec}}}$ by projecting the full 1860–2020 gappy dataset $\mathbf{X}^{\star}_{\text{ori}}$ on $\mathbf{EOF}_{\text{cal}}$, the eigenvector computed over the 1961–2018 calibration period. Two examples are available with matching dimensions: the 466-station subset of "MORA-cal X MORA-full" and the full 993-station "GridClim-full X MORA-full". In the first case, the similarity between MORA-cal X MORA-full and MORA-short demonstrates that $\widehat{\mathbf{EOF}_{\text{MORA-short}}}$ (i.e. the EOF computed from a subset of the 1860–2020 gappy $\mathbf{X}^{\star}_{\text{ori}}$ dataset, sampled at the locations of the calibration network defined in Sturm (2024b)) is equivalent to $\mathbf{EOF}_{\text{cal}}$ computed from the 1961–2018 gap-filled $\mathbf{X}^{\circ}_{\text{MORA}}$

dataset. The second case is even more conclusive: the close similarity between GridClim-full X MORA-full and MORA-full in Fig. (4) implies following equivalence:

$$\sum_{j=1}^{m_{\text{space}}} \langle \mathbf{X}^{\star}_{\text{ori}}, \widehat{\mathbf{EOF}_{\text{MORA: 1860-2020}}} \rangle \cdot \widehat{\mathbf{EOF}_{\text{MORA: 1860-2020}}}^{\dagger} \simeq \sum_{j=1}^{m_{\text{space}}} \langle \mathbf{X}^{\star}_{\text{ori}}, \mathbf{EOF}_{\text{GridClim: 1961-2018}} \rangle \cdot \mathbf{EOF}_{\text{GridClim: 1961-2018}}{}^{\dagger} \tag{12}$$

$\widehat{\overrightarrow{CI}_{\text{AM}}}$ should however not be considered equivalent to SMHI-ref, the reference climate indicator historically used by the Swedish Meteorology and Hydrology Institute. While the mathematical formula is the same (arithmetic mean of available observations), SMHI-ref is computed on 29 carefully selected synthetic (merged) long time-series with few missing values, spanning fairly uniformly over Sweden. The comparison between Fig. (3) and Fig. (8) in Sturm (2024b) shows that SMHI-ref is similar to $\widehat{\overrightarrow{CI}_{\text{EOF}}}$ presented in Fig. (3): the arithmetic average of a limited amount (29) of long time-series distributed across Sweden is representative of the EOF-based climate indicator with all (993) observation stations.

Appendix A: Empirical Orthogonal Functions: theorem and definitions

Empirical orthogonal functions (EOF) are a mathematical method to decompose a 2-dimensional matrix in two orthogonal matrices, i.e. whose column vectors are mutually uncorrelated. It is a synonym for principal component analysis (PCA).

Since the initial theorem by Autonne (1913), EOF were applied in the (presumably) first attempt of numerical weather forecasting (Richardson and Lynch, 1922; Schultz and Lynch, 2022). These initial efforts were continued to apply EOF for short-range numerical weather prediction (Wadsworth et al., 1948; Fukuoka, 1951; Lorenz, 1956).

Fundamental notions of linear algebra, and demonstration of the EOF theorem, can be found in e.g. Strang (1988, 1993, 2023). Applications of EOF methods specifically for climate and atmospheric sciences are explicited in e.g. Hannachi et al. (2023, 2007); Preisendorfer (1988); Storch et al. (1995); Storch and Zwiers (1999); Björnsson and Venegas (1997); Bretherton et al. (1992); Hartmann (2016); Wilks (2011, 2006).

We summarise hereafter the mathematical formalism of EOF, following the nomenclature in Hannachi et al. (2023, 2007); Storch and Zwiers (1999); Björnsson and Venegas (1997); Preisendorfer (1988).

A1 Standard convention for matrix dimensions: $[n_{\text{time}} \times m_{\text{space}}]$

Preisendorfer (1988); Hannachi et al. (2007) define the $[n_{\text{time}} \times m_{\text{space}}]$ observation matrix $\mathbf{X}^{\text{ori}}$. According to this convention, columns $\overrightarrow{x_j} = \mathbf{X}(:,j) \forall j \in [[1, m_{\text{space}}]]$ represents the time-series of $\mathcal{X}(t,xy)$ sampled a times $t_i \in [[1, n_{\text{time}}]]$ for location xy_j. Similarly, rows $\overrightarrow{x_i^{\text{ori}\dagger}} = \mathbf{X}(i,:)^\dagger \forall i \in [[1, n_{\text{time}}]]$ represents the spatial pattern of $\mathcal{X}(t,xy)$ sampled at the location $xy_j \in [[1, m_{\text{space}}]]$. The standard convention for the dimensions of matrix $\mathbf{X}$ is described in Eq. (A1):

$$\begin{aligned}\mathbf{X}^{\text{ori}} =& (\overrightarrow{x_1}, \ldots, \overrightarrow{x_{m_{\text{space}}}})^\dagger \\ =& \begin{bmatrix} x^{\text{ori}}_{1,1} & \cdots & x^{\text{ori}}_{1,m_{\text{space}}} \\ \vdots & \ddots & \vdots \\ x^{\text{ori}}_{n_{\text{time}},1} & \cdots & x^{\text{ori}}_{n_{\text{time}},m_{\text{space}}} \end{bmatrix}\end{aligned} \tag{A1}$$

Anomalies are computed by subtracting the time average, as indicated in Eq. (3).

The following subsections abide to the standard convention $[n_{\text{time}} \times m_{\text{space}}]$. The last subsection demonstrates the differences between the $[n_{\text{time}} \times m_{\text{space}}]$ and $[m_{\text{space}} \times n_{\text{time}}]$ conventions, as illustrated in Eq. (A13).

A2 Theorem

The theorem for the decomposition in empirical orthogonal functions (EOF) (Storch and Zwiers, 1999) is expressed as:

> Let $\mathbf{X}$ be an m-dimensional random vector with mean $\overrightarrow{\mu}$ and covariance matrix $\mathbf{S}$. Let $\lambda_1 \geq \lambda_2 \geq \cdots \geq \lambda_m$ be the eigenvalues of $\mathbf{S}$ and $\overrightarrow{e_1}, \ldots, \overrightarrow{e_m}$ be the corresponding eigenvectors of unit length. Since Σ is Hermitian, the eigenvalues λ are non-negative and the eigenvectors $\overrightarrow{e_i}$ are orthogonal.

The theorem translates to:

$$\forall k \in [[1,m]], \varepsilon_k \text{ minimises}$$

$$\varepsilon_k = \mathcal{E}\left(\| (\mathbf{X} - \overrightarrow{\mu}) - \sum_{i=1}^{k} \langle \mathbf{X} - \overrightarrow{\mu}, \overrightarrow{e_i} \rangle \overrightarrow{e_i} \|^2 \right)$$

$$\varepsilon_k = \text{var}(\mathbf{X}) - \sum_{i=1}^{k} \lambda_i$$

$$\text{var}(\mathbf{X}) = \sum_{i=1}^{m} \lambda_i \tag{A2}$$

Let $\mathbf{EOF}$ be the matrix of eigenvectors $[\overrightarrow{e_1}, \ldots, \overrightarrow{e_m}]$. By definition, eigenvectors are orthogonal (i.e. $\forall i \neq j, \langle \overrightarrow{e_i}, \overrightarrow{e_j} \rangle = 0$). Eigenvectors are chosen to be unitary (i.e. $\forall i$, $\| \overrightarrow{e_i} \| = 1$). The orthonormality of matrix $\mathbf{EOF}$ can be summarised in Eq. (A3), using the Kronecker symbol $\delta_{i,j}$:

$$\forall (i,j), \langle \overrightarrow{e_i}, \overrightarrow{e_j} \rangle = \delta_{i,j}, \text{ where } \delta_{i,j} = \begin{cases} 0 & \forall i \neq j \\ 1 & \forall i = j \end{cases}$$

$$\Leftrightarrow \mathbf{EOF} \cdot \mathbf{EOF}^\dagger = \mathcal{I}_{m_{\text{space}}}$$

$$\Leftrightarrow \mathbf{EOF}^{-1} = \mathbf{EOF}^\dagger \tag{A3}$$

To determine $\mathbf{EOF}$, we need to find the eigenvalues of the covariance matrix $\mathbf{S}$. $\mathbf{S}$, defined in Eq. (A4) has following dimension: $[m_{\text{space}} \times m_{\text{space}}]$:

$$\mathbf{S} = \sum_{t=t_1}^{t_{n_{\text{time}}}} \overrightarrow{x(t)} \cdot \overrightarrow{x(t)}^\dagger = \mathbf{X}^\dagger \cdot \mathbf{X} \tag{A4}$$

Eq. (A3) indicates that principal components $\overrightarrow{\alpha_i}$ are obtained by projecting the centred observation matrix $\mathbf{X_c}$ on their respective eigenvectors $\overrightarrow{e_i}$.

With $\mathbf{S}$ as the covariance matrix of $\mathbf{X_c}$, we can exhibit the diagonal matrix Λ with non-negative eigenvalues $\lambda_1 \geq \lambda_2 \geq \cdots \geq \lambda_m \geq 0$. According to Eq. (1), Λ and $\mathbf{S}$ are square matrices of rank m_{space}.

$$\mathbf{S} \cdot \mathbf{EOF} = \mathbf{EOF} \cdot \Lambda \Leftrightarrow \mathbf{S} = \mathbf{EOF} \cdot \Lambda \cdot \mathbf{EOF}^\dagger$$

$$\text{where } \Lambda = \text{diag}(\lambda_1, \ldots, \lambda_m) \tag{A5}$$

We furthermore can demonstrate that the i-th eigenvalue λ_k represent the variance associated to the EOF mode $(\overrightarrow{e_i}, \overrightarrow{\alpha_i})$. The portion of the variance explained by the i-th EOF mode can be expressed as r_i^2 in Eq. (A6), similar to the squared correlation coefficient used in linear regressions (Wilks, 2006).

$$\text{var}\left(\langle \mathbf{X}, \overrightarrow{e_i} \rangle\right) = \overrightarrow{e_i}^{\dagger} \cdot \mathbf{S} \cdot \overrightarrow{e_i} = \lambda_i$$
$$\Rightarrow r_i^2 = \frac{\text{var}\left(\langle \mathbf{X}, \overrightarrow{e_i} \rangle\right)}{\text{var}\left(\mathbf{X}\right)} = \frac{\lambda_i}{\sum_{k=1}^{m_{\text{year}}} \lambda_k} \tag{A6}$$

Let $\mathbf{A}$ be the matrix of associated principal component vectors $\mathbf{A} = [\overrightarrow{\alpha_1}, \ldots, \overrightarrow{\alpha_n}]^{\dagger}$. $\mathbf{A}$ is a $[n_{\text{time}} \times m_{\text{space}}]$ matrix (i.e. same dimensions as $\mathbf{X}$) and is defined in Eq. (A7):

$$\mathbf{A} = \mathbf{X} \cdot \mathbf{EOF} \Leftrightarrow \mathbf{X} = \mathbf{A} \cdot \mathbf{EOF}^{\dagger} \tag{A7}$$

Moreover, we observe that the covariance matrix of $\mathbf{A}$ is identical to the diagonal eigenvalue matrix Λ, as demonstrated in Eq. (A8).

$$\begin{aligned}\mathbf{A}^{\dagger} \cdot \mathbf{A} &= \mathbf{EOF}^{\dagger} \cdot \mathbf{X}^{\dagger} \cdot \mathbf{X} \cdot \mathbf{EOF} \\ &= \mathbf{EOF}^{\dagger} \cdot \mathbf{S} \cdot \mathbf{EOF} \\ &= \mathbf{EOF}^{\dagger} \cdot \mathbf{EOF} \cdot \Lambda \cdot \mathbf{EOF}^{\dagger} \cdot \mathbf{EOF} \\ \Leftrightarrow \mathbf{A}^{\dagger} \cdot \mathbf{A} &= \Lambda\end{aligned} \tag{A8}$$

Wilks (2006) lists different terminologies for matrices in Eq. (A3). $\mathbf{EOF}$ is commonly referred to as empirical orthogonal functions (EOF), with synonyms being eigenvectors, modes of variation, pattern vectors, or principal directions. $\mathbf{A}$ is referred to as principal components, expansion coefficients, scores, or amplitudes.

A3 Analysis of the spatial and time covariance

Let $\mathbf{X}$ be a $[n_{\text{time}} \times m_{\text{space}}]$ matrix, where $n_{\text{time}} \ll m_{\text{space}}$, centred over its 1^{st} dimension (i.e. by subtracting $\overrightarrow{\mu_{\text{time}}}$). Let $\mathbf{X'} = \mathbf{X}^{\dagger}$ be the conjugate transpose of $\mathbf{X}$ of $[m_{\text{space}} \times n_{\text{time}}$ dimension, centred over its 1^{st} dimension (i.e. by subtracting $\overrightarrow{\mu_{\text{space}}}$). If all values are real, $\mathbf{X}^{\text{T}} = \mathbf{X}^{\dagger} \forall \mathbf{X} \in \mathbb{R}^{m,n}$ Since both $\mathbf{X}$ and $\mathbf{X'}$ are both centred over their respective 1^{st} dimension, $\mathbf{X}$ and $\mathbf{X'}$ are not strictly speaking identical:

$$\begin{aligned}\mathbf{X} + \overrightarrow{\mathbf{1}_{n_{\text{year}}}}^{\dagger} \cdot \overrightarrow{\mu_{\text{time}}} &= \left(\mathbf{X'} + \overrightarrow{\mathbf{1}_{m_{\text{space}}}}^{\dagger} \cdot \overrightarrow{\mu_{\text{space}}}\right)^{\dagger} \\ \Leftrightarrow \mathbf{X} - \mathbf{X'}^{\dagger} &= \overrightarrow{\mu_{\text{space}}}^{\dagger} \cdot \overrightarrow{\mathbf{1}_{m_{\text{space}}}} - \overrightarrow{\mathbf{1}_{n_{\text{year}}}}^{\dagger} \cdot \overrightarrow{\mu_{\text{time}}}\end{aligned} \tag{A9}$$

If $\mathbf{X}$ is centred in time prior to the analysis, then:

$$\mathbf{X_c} = \mathbf{X} + \overrightarrow{\mathbf{1}_{n_{\text{year}}}}^{\dagger} \cdot \overrightarrow{\mu_{\text{time}}}$$

$$\mathbf{X_c} - \mathbf{X'_c}^{\dagger} = \mathcal{E}\left(\mathbf{X_c}^{\dagger}\right) \cdot \overrightarrow{\mathbf{1}_{m_{\text{space}}}} \tag{A10}$$

However, they can be considered as similar $\mathbf{X_c} \simeq \mathbf{X'_c}^{\dagger}$, if spatial anomalies are relatively small, i.e. $\overrightarrow{\widehat{\mu_{\text{space}}\left(\mathbf{X_c}\right)}} = \mathcal{E}\left(\mathbf{X_c}^{\dagger}\right) \ll 1$. For the sake of clarity, $\mathbf{X_c}$ is replaced by $\mathbf{X}$ in equations below.

$$\begin{cases} \mathbf{S} = \mathbf{X}^{\dagger} \cdot \mathbf{X} = \mathbf{EOF} \cdot \Lambda \cdot \mathbf{EOF}^{\dagger} \\ \mathbf{A} = \mathbf{X} \cdot \mathbf{EOF} \\ \mathbf{X} = \mathbf{A} \cdot \mathbf{EOF}^{\dagger} \end{cases} \tag{A11}$$

where $\mathbf{EOF}$, Λ are square matrices of dimension $[m_{\text{space}} \times m_{\text{space}}]$ and $\mathbf{A}$ the same dimensions as $\mathbf{X}$ ($[n_{\text{time}} \times m_{\text{space}}]$).

$$\begin{cases} \mathbf{X} \cdot \mathbf{X}^{\dagger} \simeq \mathbf{X'}^{\dagger} \cdot \mathbf{X'} = \mathbf{S'} = \mathbf{EOF'} \cdot \Lambda' \cdot (\mathbf{EOF'})^{\dagger} \\ \mathbf{A'} = \mathbf{X'} \cdot \mathbf{EOF'} \\ \mathbf{X'} = \mathbf{A'} \cdot (\mathbf{EOF'})^{\dagger} \end{cases} \tag{A12}$$

where $\mathbf{EOF'}$, Λ' are square matrices of dimension $[n_{\text{time}} \times n_{\text{time}}]$ and $\mathbf{A'}$ the same dimensions as $\mathbf{X'}$ ($[m_{\text{space}} \times n_{\text{time}}]$). Assuming that $\mathbf{X}^{\dagger} \simeq \mathbf{X'}$, we obtain $(\mathbf{A'})^{\dagger} \simeq (\mathbf{EOF'})^{\dagger} \mathbf{X}$.

$$\begin{cases} \mathbf{X} = \mathbf{A} \cdot \mathbf{EOF}^{\dagger} \\ \mathbf{X} \simeq \mathbf{EOF'} \cdot (\mathbf{A'})^{\dagger} \end{cases} \tag{A13}$$

The development above allows us to reconcile the expression of EOF analysis by Storch and Zwiers (1999) $\mathbf{X_c} = \mathbf{EOF} \cdot \mathbf{A}$ with Eq. (A7) $\mathbf{X_c} = \mathbf{A} \cdot \mathbf{EOF}^{\dagger}$ (Preisendorfer, 1988; Björnsson and Venegas, 1997; Hannachi et al., 2007). We further observe the equivalent role of $\mathbf{A'} \cong \mathbf{EOF}$ and $\mathbf{EOF'} \cong \mathbf{A}$ in Eq. (A13), bearing in mind that square matrix $\mathbf{EOF}$ is of higher rank (m_{space}) than $\mathbf{A}$'s rank (n_{time}).

Björnsson and Venegas (1997) describes $\mathbf{X}^{\dagger} \cdot \mathbf{X}$ as the *temporal covariance*, and $\mathbf{X} \cdot \mathbf{X}^{\dagger}$ as the *spatial covariance* of the observation dataset $\mathbf{X}$.

In the present case, $n_{\text{time}} \ll m_{\text{space}} \Rightarrow n_{\text{EOF}} = n_{\text{time}}$. Therefore, the principal component matrix $\mathbf{A}$ is a square matrix of rank n_{EOF} and the eigenvector matrix $\mathbf{EOF}$ has dimensions $[m_{\text{space}} \times n_{\text{EOF}}]$. The SVD decomposition is therefore equivalent to Eq. (A13), where $\mathbf{X}$ is decomposed as the product of 2 orthogonal matrices: $\mathbf{EOF'} \cong \mathbf{A}$ is a n_{time} square matrix, $\mathbf{A'} \cong \mathbf{EOF}$ a $[m_{\text{space}} \times n_{\text{time}}]$ matrix.

Eq. (A13) demonstrates the role of $[n_{\text{time}} \times m_{\text{space}}]$ versus $[m_{\text{space}} \times n_{\text{time}}]$ conventions for the definition of the covariance matrix. The goal of the present study is the *spatial covariance* in observation dataset $\mathbf{X}$, therefore we choose to exhibit the eigenvalues of covariance matrix $\mathbf{S'} = \mathbf{X} \cdot \mathbf{X}^{\dagger}$, a square matrix of rank n_{time}. Given that $n_{\text{time}} \ll m_{\text{space}}$, the covariance matrix $\mathbf{S'}$ has a smaller rank than $\mathbf{S}$. This is advantage for estimating $\widehat{\mathbf{S'}}$ from the "gappy" observation matrix $\mathbf{X}^{\star}_{\text{ori}}$ (containing missing values).

A4 EOF degeneracy

Wilks (2006) suggest several methods to assess the EOF degeneracy, by retaining significant eigenvalues (and respective eigenvectors, principal components).

Kaiser's rule, where T is a threshold constant ($T = 1$ according to Kaiser, $T = 0.7$ according to Joliffe).

$$\lambda_m > \frac{T}{n_{\text{EOF}}} \sum_{i=1}^{n_{\text{EOF}}} \text{var}\,(\overrightarrow{x_j}) \tag{A14}$$

The "broken stick model" is based on the expected length of the n^{th} longest piece of a randomly broken unit segment length. The threshold parameter $T = T(n)$ is defined as:

$$T(n) = \frac{1}{n_{\text{EOF}}} \sum_{i=n}^{n_{\text{EOF}}} \frac{1}{i} \tag{A15}$$

The threshold parameter $T = T(n)$ thus varies for each truncation level n. The retained truncation level is retained as the smallest n for which Eq. (A14) is satisfied.

North et al. (1982) proposes a rule-of-thumb: if the sampling error in the eigenvalue λ_i is comparable to the distance to a nearby eigenvalue λ_j, then the sampling error for eigenvector $\overrightarrow{e_i}$ will be comparable to the nearby eigenvector $\overrightarrow{e_j}$. n'_{EOF} represents the number of independent observations (i.e. effective sample size, or number of degrees of freedom).

$$\begin{aligned} \Delta\lambda_i &\approx \sqrt{\frac{2}{n'_{\text{EOF}}}}\lambda_i \\ \Delta\widehat{\overrightarrow{e_i}} &\approx \frac{\Delta\lambda_i}{\lambda_j - \lambda_i}\widehat{\overrightarrow{e_j}} \end{aligned} \tag{A16}$$

Thiébaux and Zwiers (1984) defines the effective sample size n'_{EOF} as a function of the auto-correlation function $\rho(k)$, computed from the k^{th} principal component $\widehat{\overrightarrow{\alpha_k}}$.

$$\begin{aligned} n'_{\text{EOF}} &= \frac{\sigma^2}{\sigma^2_{\overline{X}}} = n_{\text{EOF}} \left(\sum_{k=1}^{n_{\text{EOF}}-1} \left(1 - \frac{k}{n_{\text{EOF}}}\right) \cdot \rho(k) \right)^{-1} \\ \rho(k) &= \frac{\mathcal{E}\left(\left(\overrightarrow{X_{i+k}} - \overrightarrow{\mu}\right) \cdot \left(\overrightarrow{X_i} - \overrightarrow{\mu}\right)^* \right)}{\sigma^2} \end{aligned} \tag{A17}$$

Eq. (A17) and Eq. (A16) are combined to estimate the cutoff EOF number $N_{\text{EOF-cutoff}}$ that verifies Eq. (A18). $N_{\text{EOF-cutoff}}$ hence represents the lowest eigenvalue $\lambda_{N_{\text{EOF-cutoff}}}$ with a multiplicity of 1, i.e. non-degenerate. Degenerate eigenvalues (i.e. with a multiplicity > 1) limit the physical interpretation of individual EOFs, since physical patterns in general are not orthogonal.

$$\frac{\Delta\lambda_i}{\lambda_j - \lambda_i} < 1 \Leftrightarrow \sqrt{\frac{2}{n'_{\text{EOF}}}} \cdot \frac{\lambda_i}{\lambda_j - \lambda_i} < 1 \tag{A18}$$

Hannachi et al. (2007) defines the 95% confidence interval for eigenvalue λ_k as:

$$\frac{\Delta\lambda_i}{\lambda_i} \approx 1 \pm \sqrt{\frac{2}{n'_{\text{EOF}}}} \tag{A19}$$

Appendix B: Mathematical notations

The list below summarises the mathematical notations used in this study, in accordance with Storch and Zwiers (1999).

- The notation $\overrightarrow{X}$ represents (row) vectors, and $\mathbf{X}$ denotes matrices.
- $\mathbf{X}^\star$ denotes a "gappy" matrix (i.e. with missing values), $\mathbf{X}^\circ$ a complete matrix.
- $\overrightarrow{\mathbf{1}_n} = [1, \ldots, 1]$ represents a n-dimension (row) unit-vector, $\mathcal{I}_n$ the identity matrix of rank n.
- The *complex conjugate* of a complex number a is noted a^*: $\forall a \in \mathbb{C}$, $a^* = \Re(a) - i \cdot \Im(a)$.
- The *transpose* of a vector or matrix $\mathbf{A}$ is noted $\mathbf{A}^{\mathrm{T}}$, defined as $\forall (i,j) \in ([[1,n]],[[1,m]])$, $A^{\mathrm{T}}_{i,j} = A_{j,i}$.
- The *conjugate transpose* of a matrix or vector $\mathbf{A}$ is noted $\mathbf{A}^\dagger = \mathbf{A}^{\mathrm{T}*} = \mathbf{A}^{*\mathrm{T}}$
- For *real* vectors or matrices, the notation can be simplified: $\forall \mathbf{A} \in \mathbb{R}^{(n,m)}$, $\mathbf{A} = \mathbf{A}^*$, $\mathbf{A}^{\mathrm{T}} = \mathbf{A}^\dagger$
- The *dot product* (also scalar or inner product) of two vectors is noted $\langle \overrightarrow{a}, \overrightarrow{b} \rangle = \overrightarrow{b}^\dagger \overrightarrow{a} = \sum a_i b_i^*$.
- The *norm* of vector $\overrightarrow{a}$ is noted $\| \overrightarrow{a} \| = \sqrt{\langle \overrightarrow{a}, \overrightarrow{a} \rangle}$
- For "gappy" observation datasets $\mathbf{X}^\star$, $\mathcal{D}$ represents *ensemble* of elements non-missing values. The matrix $\mathcal{D}$ (with same dimension as $\mathbf{X}^\star$) is represented as a collection of vectors $\mathcal{D} = \left[\overrightarrow{\mathcal{D}_1}, \ldots, \overrightarrow{\mathcal{D}_{n_{\text{year}}}}\right]^\dagger$ where $\overrightarrow{\mathcal{D}_i}$ represents all non-missing time-steps t_i, $\forall [[1, n_{\text{year}}$ at location xy_j. $|\overrightarrow{\mathcal{D}_i}|$ represents the number of elements in $\overrightarrow{\mathcal{D}_i}$. $\overrightarrow{\mathcal{D}_i} \cap \overrightarrow{\mathcal{D}_j}$ represents the intersection of $\overrightarrow{\mathcal{D}_i}$ and $\overrightarrow{\mathcal{D}_j}$, i.e. where the subset where non-missing elements in columns i and j.
- The expectation of n-element vector $\overrightarrow{X}$ is noted $\mathcal{E}\left(\overrightarrow{X}\right) = \frac{1}{n} \sum_{i=1}^{n} x_i$
- $\delta_{i,j}$ represents the *Kronecker symbol*, defined as $\forall i = j$, $\delta_{i,j} = 1$, $\forall i \neq j$, $\delta_{i,j} = 0$.

References

Anonymous, R.: Reviewer's comment on "Spatially aggregated climate indicators over Sweden (1860–2020), Part 1: Temperature", https://doi.org/10.5194/egusphere-2024-582-RC1, 2024a.

Anonymous, R.: Reviewer's comment on "Spatially aggregated climate indicators over Sweden (1860–2020), Part 1: Temperature", https://doi.org/10.5194/egusphere-2024-582-RC2, 2024b.

Autonne, L.: Sur les matrices hypohermitiennes et les unitaires, Comptes Rendus de l'Académie des Sciences, 156, 858–860, 1913.

Björnsson, H. and Venegas, S. A.: A manual for EOF and SVD analyses of climatic data, CCGCR Report 97, Centre for Climate and Global Change Research – McGill University, http://www.geog.mcgill.ca/gec3/wp-content/uploads/2009/03/Report-no.-1997-1.pdf, 1997.

Bretherton, C. S., Smith, C., and Wallace, J. M.: An Intercomparison of Methods for Finding Coupled Patterns in Climate Data, Journal of Climate, 5, 541–560, https://doi.org/10.1175/1520-0442(1992)005<0541:AIOMFF>2.0.CO;2, publisher: American Meteorological Society Section: Journal of Climate, 1992.

Fukuoka, A.: A study on 10-day forecast – A synthetic report, Geophysical Magazine, 22, 177–208, https://cir.nii.ac.jp/crid/1520573330554458880, publisher: Tokyo : Japan Meteorological Agency, 1951.

Hannachi, A., Jolliffe, I. T., and Stephenson, D. B.: Empirical orthogonal functions and related techniques in atmospheric science: A review, International Journal of Climatology, 27, 1119–1152, https://doi.org/10.1002/joc.1499, _eprint: https://onlinelibrary.wiley.com/doi/pdf/10.1002/joc.1499, 2007.

Hannachi, A., Finke, K., and Trendafilov, N.: Common EOFs: a tool for multi-model comparison and evaluation, Climate Dynamics, 60, 1689–1703, https://doi.org/10.1007/s00382-022-06409-8, 2023.

Hartmann, D. L.: Objective analysis, no. 552 in Atmospherical Sciences, University of Washington, Washington, https://www.atmos.washington.edu/~dennis/552/, 2016.

Joelsson, L. M. T., Engström, E., and Kjellström, E.: Homogenization of Swedish mean monthly temperature series 1860–2021, International Journal of Climatology, 43, 1079–1093, https://doi.org/10.1002/joc.7881, _eprint: https://onlinelibrary.wiley.com/doi/pdf/10.1002/joc.7881, 2023.

Lorenz, E. N.: Empirical Orthgonal Functions and Statistical Weather Prediction, Scientific Report 1, Massachusetts Institute of Technology (MIT), Dpt. of Meteorology, http://muenchow.cms.udel.edu/classes/MAST811/Lorenz1956.pdf, 1956.

North, G. R., Bell, T. L., Cahalan, R. F., and Moeng, F. J.: Sampling Errors in the Estimation of Empirical Orthogonal Functions, Monthly Weather Review, 110, 699–706, https://doi.org/10.1175/1520-0493(1982)110<0699:SEITEO>2.0.CO;2, publisher: American Meteorological Society Section: Monthly Weather Review, 1982.

Preisendorfer, R. W.: Principal Component Analysis in Meteorology and Oceanography, Elsevier, Amsterdam, ISBN 978-0-444-43014-4, https://www.researchgate.net/profile/Curtis-Mobley-2/publication/44529688_Principal_component_analysis_in_meteorology_and_oceanography_by_Rudolph_W_Preisendorfer_posthumously_compiled_and_edited_by_Curtis_D_Mobley/links/541875e90cf2218008bf3da1/Principal-component-analysis-in-meteorology-and-oceanography-by-Rudolph-W-Preisendorfer-posthumously-compiled-and-edited-by-Curtis-D-M pdf, google-Books-ID: Mt_scAAACAAJ, 1988.

Quayle, R. G., Easterline, D. R., Karl, T. R., and Hughes, P. Y.: Effects of Recent Thermometer Changes in the Cooperative Station Network, Bulletin of the American Meteorological Society, 72, 1718–1724, https://doi.org/10.1175/1520-0477(1991)072<1718:EORTCI>2.0.CO;2, publisher: American Meteorological Society Section: Bulletin of the American Meteorological Society, 1991.

Richardson, L. F. and Lynch, P.: Weather Prediction by Numerical Process, Monthly Weather Review, https://doi.org/10.1017/cbo9780511618291, publisher: Cambridge University Press, 1922.

Schultz, D. M. and Lynch, P.: 100 Years of L. F. Richardson's Weather Prediction by Numerical Process, Monthly Weather Review, 150, 693–695, https://doi.org/10.1175/MWR-D-22-0068.1, publisher: American Meteorological Society Section: Monthly Weather Review, 2022.

Storch, H. v. and Zwiers, F. W.: Statistical Analysis in Climate Research, Cambridge University Press, Cambridge, ISBN 978-0-521-01230-0, https://doi.org/10.1017/CBO9780511612336, 1999.

Storch, H. v., Bürger, G., Schnur, R., and Storch, J.-S. v.: Principal Oscillation Patterns: A Review, Journal of Climate, 8, 377–400, https://doi.org/10.1175/1520-0442(1995)008<0377:POPAR>2.0.CO;2, publisher: American Meteorological Society Section: Journal of Climate, 1995.

Strang, G.: Linear Algebra and Its Applications, Cengage Learning, Belmont, CA, 4th edition edn., ISBN 978-0-03-010567-8, https://anandinstitute.org/pdf/linearapplication.pdf, 1988.

Strang, G.: The Fundamental Theorem of Linear Algebra, The American Mathematical Monthly, https://doi.org/10.2307/2324660, publisher: Taylor & Francis, 1993.

Strang, G.: Introduction to Linear Algebra, Wellesley-Cambridge Press, Wellesley, Mass, 6th edition edn., ISBN 978-1-73314-667-8, https://math.mit.edu/~gs/linearalgebra/ila6/indexila6.html, 2023.

Sturm, C.: Spatially aggregated climate indicators over Sweden (1860 – 2020), part 2: Precipitation, EGUsphere, pp. 1–38, https://doi.org/10.5194/egusphere-2024-940, publisher: Copernicus GmbH, 2024a.

Sturm, C.: Spatially aggregated climate indicators over Sweden (1860 – 2020), Part 1: Temperature, EGUsphere, pp. 1–40, https://doi.org/10.5194/egusphere-2024-582, publisher: Copernicus GmbH, 2024b.

Thiébaux, H. J. and Zwiers, F. W.: The Interpretation and Estimation of Effective Sample Size, Journal of Climate and Applied Meteorology, 23, 800–811, https://doi.org/10.1175/1520-0450(1984)023<0800:TIAEOE>2.0.CO;2, 1984.

Thomson, R. E. and Emery, W. J.: Chapter 4 - The Spatial Analyses of Data Fields, in: Data Analysis Methods in Physical Oceanography (Third Edition), edited by Thomson, R. E. and Emery, W. J., pp. 313–424, Elsevier, Boston, ISBN 978-0-12-387782-6, https://doi.org/10.1016/B978-0-12-387782-6.00004-1, 2014.

Wadsworth, G. P., Bryan, J. G., and Gordon, C.: Short range and extended forecasting by statistical methods, US Air Force, Air Weather Service Tech. Report, 1948.

Wilks, D. S.: Statistical Methods in the Atmospheric Sciences, vol. 91 of *Internationbal Geophysics Series*, Academic Press, Amsterdam, 2nd ed. edn., ISBN 978-0-12-751966-1, https://sunandclimate.files.wordpress.com/2009/05/statistical-methods-in-the-atmospheric-sciences-0127519661.pdf, google-Books-ID: _vSwyt8_OGEC, 2006.

Wilks, D. S.: Statistical Methods in the Atmospheric Sciences, Academic Press, ISBN 978-0-12-385022-5, https://sunandclimate.wordpress.com/wp-content/uploads/2009/05/statistical-methods-in-the-atmospheric-sciences-0127519661.pdf, google-Books-ID: IJuCVtQ0ySIC, 2011.

Zhang, Z. and Moore, J. C.: Chapter 6 - Empirical Orthogonal Functions, in: Mathematical and Physical Fundamentals of Climate Change, edited by Zhang, Z. and Moore, J. C., pp. 161–197, Elsevier, Boston, ISBN 978-0-12-800066-3, https://doi.org/10.1016/B978-0-12-800066-3.00006-1, 2015.